Clays and Clay Minerals, Vol. 56, No. 2, 144–154, 2008.

MICROSTRUCTURE OF ORGANO-BENTONITES IN WATER AND THE EFFECT OF STERIC HINDRANCE ON THE UPTAKE OF ORGANIC COMPOUNDS

JIANXI ZHU, LIZHONG ZHU*, RUNLIANG ZHU, AND BAOLIANG CHEN

Department of Environmental Science, Xixi Campus, Zhejiang University, 148 Tianmushan Street, Hangzhou, Zhejiang, 310028, China

Abstract—To further elucidate adsorption-to-partition transitional mechanisms which have been proposed previously for organo-bentonites with different surfactant loadings, the structural characteristics of interlayer surfactant aggregates on organo-bentonite with different surfactant cetyltrimethylammonium bromide loading levels (0.20−2.56 times cation exchange capacity, CEC) have been investigated by *in situ* X-ray diffraction (XRD) and Fourier Transform Infrared (FTIR) spectroscopy. The sorption properties and the structure of the clay interlayers changed according to the type of surfactant, the surfactant loading level, and the state of hydration in the clays. Based on the sorption of nitrobenzene, phenol, and aniline to organo-bentonites, the contaminant sorption coefficients (K_{sf}), normalized with the organic carbon content, show a remarkable dependence on surfactant loading levels. The K_{sf} values first increased with surfactant loading until reaching a maximum at 1.0 to 1.2 times the CEC, and then decreased. According to the theoretical calculation of the volume fractions relating to the interlamellar space, the interlamellar microenvironment became a more hydrophobic medium, contributing to the dissolution of organic contaminants, as the surfactant loading increased from 0.20 to 2.56 times the CEC. However, the increase in packing density (ρ) for the intercalates, and induced steric hindrances both affect the result in terms of a reduction in the accessible free space where the organic contaminants can be located, which might be a negative factor in the sorption capacity.

Key Words—Organo-bentonite, Microstructure, Steric Hindrance Mechanisms, Sorption Efficiency, Surfactant Loadings.

INTRODUCTION

Growing concerns about the effects of hydrophobic organic compounds (HOCs) in waste water and in contaminated soil have led to the development of modified clay minerals for pollution-control and remediation purposes. Previous studies have demonstrated that cationic surfactants can be intercalated into the interlayer spaces of swelling layer silicates to enhance contaminant retention and retard contaminant migration (Jaynes and Boyd, 1991; Zhang *et al.*, 1993; Xu and Boyd, 1995; Lee and Kim, 2002; Zhu *et al.*, 2003b). Sorption of neutral organic contaminants by long-chain, surfactant-modified organo-clays is controlled primarily by solute partitioning, which is characterized by an essentially linear isotherm dependence of sorption on organic content (Boyd *et al.*, 1988). In more recent studies, the phenomenon of sorbates assisting in further sorption was observed (Dékány, Sheng, Morland, Xu, Slade, *etc*). When the amount of long-chain surfactant added exceeds the CEC of montmorillonite, completion of the cation exchange reaction in the interlayer is followed by excess surfactant cations being sorbed on the surface. The binding of the excess cations involves ion-dipole and ion-ion interactions in addition to van der Waals forces (Jaynes and Boyd, 1991; Yariv and Cross, 2002). Sheng and Boyd (Sheng *et al.*, 1996a, 1996b; Sheng and Boyd, 2000) attributed the uptake of neutral organic contaminants in binary solute systems from water by hexadecyltrimethylammonium clays to the occurrence of multiple sorption mechanisms, including solvation with ammonium cations and mineral surfaces, and partition with the HDTMA organic phase. In this situation, the organic matter-normalized, organic-solute sorption coefficients (K_{sf}) usually varied significantly with the surfactant loadings (Zhu *et al.*, 2003b), For example, Li and Bowman (1998) observed a decrease in the solute K_{sf} values with an increase in sorbed cetyltrimethyl ammonium when the surfactant was loaded at a rate >1.5CEC, and constant K_{sf} when surfactant loading was $\leqslant$1.0CEC. Chen *et al.* (2005) suggested that the sorption process of HOCs was influenced by the amount of sorbed organic cation and its composition, and configurations of the sorbed organic cation. These results imply that the sorption process was influenced greatly by the surfactant loading levels, especially the quantity of surfactant sorbed in excess of the CEC of the clay.

As is well known, long alkyl chains usually congregate into intercalates at the solid-water interface, even at very small surfactant coverage (Kung and Hayes, 1993). Here, 'solloid' is a general term used for those surfactant aggregates on solid surfaces including all sorts of adsorbed surfactant layer structures such as

* E-mail address of corresponding author:
zlz@zju.edu.cn
DOI: 10.1346/CCMN.2008.0560202

monolayers, bilayers, hemimicelles, admicelles, and small-surface micelles (Fan *et al.*, 1997). There has been a large number of recent studies, with different models proposed for the progress of surfactants adsorbed on charged solid surfaces (Somasundaran and Kunjappu, 1989; Kung and Hayes, 1993; Fan *et al.*, 1997; Bakker *et al.*, 2000; Somasundaran and Huang, 2000). For example, Harwell (1985), Wu *et al.* (1987), and Somasundaran and Kunjappu (1989) proposed the surface bilayer model and the reverse-orientation model for surfactant aggregates on solid surfaces. The difference between the two models is that the former owns the complete bilayer, and the latter is a paraffin-like structure where the alkyl chains interact *via* van der Waals forces and the cationic head groups alternate to different sides of the structure. In these models, the adsorption isotherms and surfactant aggregate structures were different, and increased surfactant loading resulted in changes in the organic phase structure (Lagaly, 1976; Dékány *et al.*, 1986b; Slade and Gates, 2004a).

Interlayer organic surfactants within dry organic bentonites have been studied in detail using different spectroscopic and microscopic techniques (Lagaly, 1981; Vaia *et al.*, 1994; Theng *et al.*, 1998; Wang *et al.*, 2000; He *et al.*, 2004; Zhu *et al.*, 2005) and molecular simulation methods (He *et al.*, 2005). With increasing organic load, the surfactants changed their molecular arrangement from monolayer to bilayer, then to either a pseudo-bilayer or a paraffin-like structure (Lagaly, 1981). Their molecular environment transforms from a liquid-like state to a solid-like state (Vaia *et al.*, 1994) while the conformation varied from *gauche* to all-*trans* (Wang *et al.*, 2000; He *et al.*, 2004; Zhu *et al.*, 2005). However, previous information about the properties of interlayer organic phases was obtained from dried powder of organic bentonite, which may change in the more likely aqueous state. Xu and Boyd (1995) and Kung and Hayes (1993) pointed out that the organic clay microstructures and surfactant orientation deduced from the organic clay powder do not represent those in aqueous medium. Generally, the montmorillonites and their organic-surfactant derivatives swell and disaggregate in organic liquids and mixtures, the organo-montmorillonites swell in organic medium due to the sorption of interlamellar liquid. Over the past two decades, Dékány and co-workers have studied the liquid sorption and immersional wetting properties of hydrophilic/hydrophobic solid surfaces in binary liquid mixtures such as the methanol-benzene mixture and 1-pentanol-water mixture (Dékány *et al.*, 1975, 1985, 1986a, 1986b, 1989, 1994, 1996; Szántó *et al.*, 1986; Dékány, 1992, 1994; Döring *et al.*, 1993; Marosi *et al.*, 1994). The interlamellar structure and the alkyl-chains arrangement of organo-montmorillonite in liquid mixtures were described, as were the relationships between the volume of the adsorbed phase and the total interlayer volume or interlayer spacing (obtained from XRD data). Up to now, the exact structure and intercalation state of adsorption layers of organic cations in water has not been studied in detail. This, in spite of the fact that organo-bentonites have been investigated extensively as sorbents for organic pollutants in water.

The main objective of the current study is to relate the *in situ* structural characteristics of surfactant intercalates with the sorption characteristics of organo-bentonites. To this end, the sorption of nitrobenzene, phenol, and aniline to organo-bentonites with different levels of surfactant loading were investigated. The interlayer organic phases (intercalates) of the wet organo-bentonites were examined by XRD and FTIR.

MATERIALS AND METHODS

Materials

Aniline, phenol, and nitrobenzene were of analytical grade and were used without further treatment. Bentonite (NM-Bent) was selected as the model mineral. It was obtained from Inner Mongolia, China; its XRD patterns showed it to be a very pure montmorillonite (>95%) containing quartz as an impurity (<5%). Its structural formula can be expressed as $Na_{0.02}K_{0.02}Ca_{0.39}[Fe_{0.45}Mg_{1.10}Al_{2.51}][Si_{7.91}Al_{0.09}]O_{20}(OH)_4{\cdot}nH_2O$, calculated from the oxides analysis of the starting sample. The net charge of the montmorillonite interlayer is 0.82 per unit cell. The surfactant used in this study was cetyltrimethylammonium bromide (CTMAB) with a purity of 99%. Aniline, phenol, and nitrobenzene, with different polarities, were used to probe the microenvironment of the sorbed surfactant in the interlayer space of the clay. The octanol-water partition coefficients ($\log K_{ow}$) of aniline, phenol, and nitrobenzene are 0.9, 1.46, and 1.85, respectively, and their respective aqueous solubilities are 34.160, 80.190, and 1936 μg mL^{-1} at 25ºC.

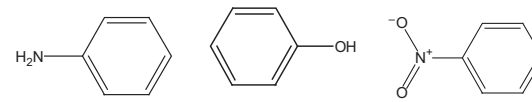

Aniline Phenol Nitrobenzene

The air-dried bentonite sample was sieved to obtain particles of <165 μm, which were used in all experiments. The Brunauer Emmett Teller (BET)-N_2 surface area of bentonite, organic-carbon content (f_{oc}), and CEC are 55 m^2/g, 0.04%, and 1.084 mol/kg, respectively.

Analytical methods

The quantities of aniline, phenol, and nitrobenzene in aqueous solutions were quantified by ultraviolet spectrophotometry at absorbance wavelengths of 230, 210, and 268 nm, respectively. The pH values of the analyte solutions were maintained at between 7 and 8. The organic carbon content was determined using a Shimadzu SSM-5000A TOC analyzer at 50% relative humidity at 25ºC.

Preparation of organic bentonites

The preparation of organic bentonite hybrids was carried out as follows: 20 g of bentonite were first dispersed in ~200 mL of deionized water and then the desired amount of CTMAB was added slowly. The amount of CTMAB varied from 0.2 to 3.0 times the CEC of bentonite. The reaction mixtures were stirred at 60ºC for 2 h. All products were washed with water until bromide anions were undetectable with $AgNO_3$. The solution and solid phase were separated by centrifugation at 4000 rpm for 10 min at 25ºC. Part of the solid was dried at 70ºC and ground in an agate mortar to pass through a 165 μm sieve, and the organic carbon contents of the solution were measured in a TOC analyzer, determining the exact loading level of CTMAB. The organic bentonite prepared at 0.2 times the CEC of the bentonite was denoted as 0.2CEC and the other loading treatments were named accordingly.

Characterization of in situ XRD and FTIR

The air-dried and water-saturated samples of bentonite and organic clays (*i.e.* 0.2−3.0CEC) were characterized by XRD and FTIR spectroscopy. The XRD patterns were recorded using a Rigaku D/max-2550PC diffractometer with CuKα radiation at a relative humidity of 60−70% and at 25ºC, using a scanning rate of 4º2θ min^{-1}. The analysis of the air-dried samples followed ordinary powder diffraction methods. For wet samples, the initial suspension was centrifuged and the residue, in paste form, was placed on a support and immediately subjected to XRD measurement. The interlayer heights for various clay samples were determined by subtracting the van der Waals thickness of a silicate layer (0.96 nm) from the measured basal spacings (d_{001}). X-ray diffraction data revealed that the original bentonite was well crystallized. No evidence of other crystallite phases was detected except for a little quartz. The FTIR spectra of aqueous samples were recorded in the region 4000−400 cm^{-1} using a Bruker Vector-22 FTIR spectrometer. The organic bentonite samples for the FTIR analysis were prepared as diluted slurries and daubed on a sample cell made from two CaF_2 crystals. The FTIR spectra were obtained by accumulating at least 128 scans at a resolution of 4 cm^{-1} using Happ-Genzel apodization.

Sorption of organic contaminants onto organo-bentonites

Various quantities of organic pollutant were added to the 25 mL Erlenmeyer flasks with glass caps, which each contained 0.2 g of organic bentonite (0.2−3.0CEC). The flasks were shaken for 12 h at 25±0.5ºC on a gyratory shaker at 150 rpm to reach an equilibrium state. The liquid and solid components were then separated by centrifugation at 4000 rpm for 10 min. The supernatants were removed and analyzed for specific organic pollutants by UV. The concentrations of the organic pollutants were calculated from the final UV readings while the sorbed amounts were evaluated from the difference between the initial and final solute concentrations.

RESULTS AND DISCUSSION

Sorption of CTMAB onto bentonite

Based on the organic-carbon contents in the supernatants during preparation of organic bentonites, the amounts of surfactant adsorbed were calculated, and the exact loading level of CTMAB and TOC of the organic bentonites were derived. The results are presented in Table 1. In the case of sorbed levels (C_{sorbed}/CEC) of <1.2, nearly 100% of the $CTMA^+$ was taken up by bentonite.

At greater CTMAB loading levels, C_{sorbed}/CEC increased gradually, and the final saturation corresponded to ~2.56 times the CEC of the bentonite. This is similar to the reported isotherm for CTMAB sorbed by Ca^{2+}-montmorillonite. Xu *et al.* (1997) and Lee and Kim (2002) also found that the maximum uptake of CTMAB occurred at ~2.56 times the CEC. The surfactant uptake by bentonite proceeded *via* two steps, initially by cation exchange and then by a co-adsorption process. Both processes contribute to the overall uptake of long-alkyl-chain organic cations by clays (Lagaly, 1981; Xu and Boyd, 1995; Xu *et al.*, 1997; Lee and Kim, 2002; Zhu *et al.*, 2003b). The co-adsorption processes of surfactant salt molecules presumably result from the non-electrostatic interactions (*e.g.* hydrophobic bonding) between the alkyl tails of the organic cations, bound by their head groups to the clay surfaces as a result of cation exchange, and the alkyl tails of the organic salt molecules. In the case of loading levels of <1.2CEC, cation exchange was apparently the primary mechanism for $CTMA^+$ sorption. In the region 1.2−2.0CEC, both cation exchange and non-electrostatic interactions could have taken place. But the contribution from the cation exchange would become relatively insignificant with increased loading level. Starting from the sorbed level of 2.0 times the CEC, non-specific binding, such as ion-dipole and ion-ion interactions, in addition to van der Waals forces, was presumably the main mechanism until the $CTMA^+$ sorption reached a plateau (*i.e.* C_{sorbed} = 2.56CEC).

In situ structural characteristics of intercalates

The structure of the organic bentonite was strongly influenced by surfactant-uptake mechanisms and the loading levels. As far as we know, there is little *in situ* information about the microstructure and molecular environment of surfactant aggregates (intercalates) in aqueous suspension, which is important in understanding transitional sorption mechanisms by organo-bentonites in water.

It is important to understand the microstructure characteristics of the interlayer intercalates, including

Table 1. Characterization results of the original and organic bentonites.

Sample	f_{oc} (%)	C_{sorbed}/CEC	$d_{001\ (dried)}$ (nm)	$d_{001\ (moist)}$ (nm)	ν_{as} ($-CH_2$) (cm^{-1})	ν_s ($-CH_2$) (cm^{-1})
NM	0.04	–	1.52	1.84	–	–
0.2CEC	4.7	0.199	1.51	1.98	2924	2853
0.4CEC	9.1	0.399	1.50	3.02	2920	2851
0.6CEC	12.6	0.599	1.62	3.13	2919	2850
0.8CEC	16.6	0.799	1.80	3.15	2918	2850
1.0CEC	20.7	0.999	1.85	3.25	2919	2850
1.2CEC	22.3	1+0.199	1.97	3.50	2918	2850
1.4CEC	25.4	1+0.393	2.74	3.70	2919	2851
1.6CEC	26.1	1+0.592	3.34	3.87	2918	2850
1.8CEC	28.7	1+0.783	3.50	4.08	2918	2850
2.0CEC	30.0	1+0.979	3.81	4.12	2918	2850
2.5CEC	33.0	1+1.451	3.80	4.12	2919	2850
3.0CEC	34.1	1+1.562	3.80	4.20	2918	2850
CTMAB (monomer)	–	–	–	–	2930	2860
CTMAB (micelle)	–	–	–	–	2923	2853
CTMAB (solid)	–	–	–	–	2918	2850

f_{oc}: organic carbon content; C_{sorbed}/CEC: saturated CEC by the intercalated surfactants; $d_{001\ (dried)}$: basal spacings of the dried samples; $d_{001\ (moist)}$: basal spacings of the moist samples; ν_{as} ($-CH_2$): antisymmetric $-CH_2$ stretching vibration for the intercalated surfactant in the moist organic bentonites; ν_s ($-CH_2$): symmetric $-CH_2$ stretching vibration for the intercalated surfactant in the moist organic bentonites.

charge density, surfactant packing density (hydrocarbon density), volumes of surfactant, and water in the interlayer space, in order to establish the process by which organic contamination sorbed onto organo-bentonite. These micro-environmental properties can be evaluated according to the charge density of the clay layer, actual quantity of surfactant loading, and the height of the interlayer space combined with the configuration of the surfactant molecules. All these parameters can be obtained by different analytical techniques. For example, the basal spacing of organo-bentonite (d_{001}) can be obtained *via* XRD and the quantity of loaded surfactant can be determined by measuring the total organic carbon (TOC) of the residual concentration of supernatant during preparation of the organo-clay. The structural parameters calculated from the crystal chemistry of interlayer organic phases will contribute to a better understanding of the relationship between the microstructure of the interlayer intercalates within organo-bentonites and their sorption ability for organic contaminants in water.

The structural characteristics of $CTMA^+$/CTMAB clay intercalates were evaluated by XRD and FTIR methods on samples in a hydrated state. The XRD patterns of bentonite and 0.2−3.0CEC samples are listed in Tables 1 and 2. For the dried and hydrated organo-bentonites, the measured basal spacings depended on surfactant loadings (Figure 1). It can be seen that d_{001} reaches 3.0 nm for moist organo-bentonite at a very small surfactant loading. The difference in interlayer spacing between the moist and dried, original bentonites ($\Delta H = d_{001\ wet} - d_{001\ dry}$) is 0.32 nm. The ΔH value increased to 0.47 nm for 0.2CEC organo-bentonites, jumped to 1.5 nm with loadings between 0.4 and 1.2 × CEC, and then decreased rapidly to 0.31 nm at 2.0CEC. The ΔH values for organo-bentonite with large surfactant loadings (*i.e.* 2.0CEC−3.0CEC) are consistent with that of original bentonite. These observations indicated that water molecules might play an important role in regulating the microenvironment, even at extremely large surfactant loads. In this way, water molecules contribute to the multiple properties of the microenvironments. Consequently, with the increase of surfactant loading levels for dried organic bentonites, the

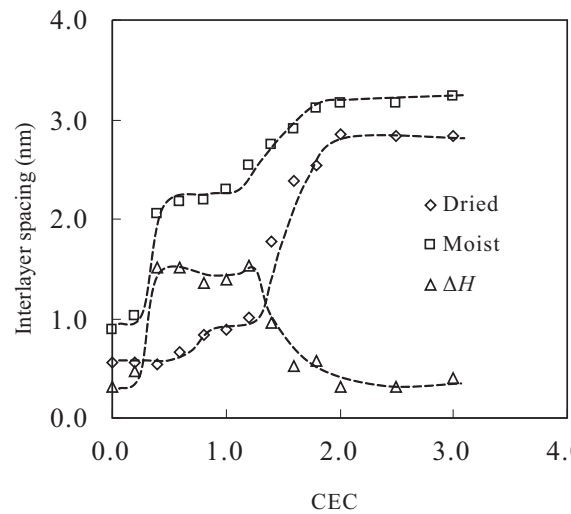

Figure 1. Interlayer spacing ($\Delta d = d_L - 0.96$) for the dried and moist, organo-bentonites; ΔH was the difference in interlayer spacing between the moist and dried organo-bentonites. The curves are included to aid the eye.

Table 2. Calculated results of interlayer structure in a single cell of the original bentonite and of the organo-bentonites.

Sample	Δd (nm)	N	V_{IS} (nm^3)	$V_{surfactant}$ (nm^3)	V_{H_2O} (nm^3)	$V_{H_2O}/CTMA^+$	$M_{H_2O}/CTMA^+$	ρ (g/cm^3)
NM	0.88	–	0.41	–	0.41	–		
0.2CEC	1.02	0.16	0.48	0.10	0.38	3.80	204.30	0.16
0.4CEC	2.06	0.33	0.96	0.20	0.76	3.80	204.30	0.16
0.6CEC	2.17	0.49	1.02	0.31	0.71	2.29	123.14	0.23
0.8CEC	2.19	0.66	1.02	0.41	0.62	1.51	81.30	0.30
1.0CEC	2.29	0.82	1.07	0.51	0.56	1.10	59.03	0.33
1.2CEC	2.54	0.98	1.19	0.61	0.58	0.95	51.12	0.39
1.4CEC	2.74	1.14	1.28	0.71	0.57	0.80	43.16	0.44
1.6CEC	2.91	1.31	1.36	0.81	0.55	0.68	36.51	0.48
1.8CEC	3.12	1.46	1.46	0.91	0.55	0.60	32.49	0.52
2.0CEC	3.16	1.62	1.48	1.01	0.47	0.47	25.02	0.57
2.5CEC	3.16	2.01	1.48	1.25	0.23	0.18	9.89	0.73
3.0CEC	3.24	2.10	1.52	1.31	0.21	0.16	8.62	0.75

Δd: interlayer spacing for the moist samples, obtained by subtraction of the thickness of the clay layer from d_{001}; N: the number of surfactant molecules or cations per unit cell; V_{IS}: volume of interlayer space per unit cell; $V_{surfactant}$: volume of surfactant per unit cell when the loading levels are = 1.0CEC, the $V_{surfactant} = V_{CTMA^+}$; when the loading levels are >1.0CEC, $V_{surfactant} = V_{CTMA^+} + V_{CTMAB}$; V_{H_2O}: volume of water per unit cell; $V_{H_2O/CTMA^+}$: volume ratio of water and surfactant in the bentonite interlayer; $M_{H_2O/CTMA^+}$: molecular ratio of water to surfactant in the bentonite interlayer; ρ: packing density of the intercalated surfactants.

arrangement models changed from monolayers to bilayers, and then to pesudotrimolecular layers; the paraffin layers were not suitable for moist organic bentonites.

Due to the favorable hydrophobic interactions in the presence of water, the methylene chains form an aggregate structure in the interlayer space. As a result, the values of d_{001} increase gradually with increase in surfactant loading. Various models for the surfactants in the clay interlayer space have been proposed on the basis of basal spacings of organo-clays and the dimension of the surfactant (Lagaly, 1982; Favre and Lagaly, 1991; Zhu *et al.*, 2003a). According to the XRD data and the dimensions of the $CTMA^+$ (Figure 2a(1)), special arrangements of the CTMAB surfactant in moist organo-bentonites with different surfactant loading levels are proposed in Figure 2b. In this model, the long axes of the alkyl chains were perpendicular, not inclined, to the O-plane surfaces when the surfactant loading levels were high; the alkyl chains overlap each other and form an interpenetrating monolayer arrangement (Dékány *et al.*, 1986b).

When the surfactant is added to the aqueous bentonite suspension, all exchange sites are potentially available to take part in an exchange reaction. If the quantity of CTMAB added was less than the CEC (*e.g.* 0.2CEC), only some of the interlayer inorganic ions can be exchanged by surfactant cations. The resulting interlayer space is therefore occupied by $CTMA^+$, Ca^{2+}, Na^+, Mg^{2+}, and H_2O. The interlayer spacing (Δd) is 1.02 nm and the $CTMA^+$ could only lie parallel to the host silicate planes (Figure 2b(1)). At 0.4−1.2CEC, the spacings of ~2.0−2.5 nm are roughly the length of $CTMA^+$. Hence, a possible arrangement could involve the $CTMA^+$ head groups being anchored on the clay surface and the long alkyl chains having a maximum angle of 90° with respect to the clay surface (Figure 2b(2)). When the loading level exceeds 1.0CEC, the sorbed organic cations and surfactant salt molecules form the special interfingered, bi-molecular layer (Figure 2b(3)) (Lee *et al.*, 1989; Rennie *et al.*, 1990; Li and Bowman, 1998). The interlayer organic phases might be divided into two regions: (1) outer region (*i.e.* closest to the clay surfaces); and (2) inner region (*i.e.* well within the interlayer space). The outer region, which extends ~0.5 nm from the clay surfaces, contains the trimethylammonium head groups and, if loaded in excess of the CEC, also contains Br^- ions, while the innermost region, ~2 nm thick, contains only tails of the alkyl chains (Slade and Gates, 2004b). Due to the incomplete bilayer formed in the structure, this partial or 'patchy' bilayer model is more like a reverse-orientation model than a bilayer model (Somasundaran and Kunjappu, 1989).

Configurations of $CTMA^+$/CTMAB in the intercalates. According to the study reported by Kung and Hayes (1993), *in situ* FTIR spectroscopy was suitable for identifying structural changes of surfactant aggregates occurring as a function of surfactant surface coverage and degree of hydration. The wavenumbers of the antisymmetric and symmetric -CH_2- stretching vibrations of CTMAB and organo-bentonites are summarized in Table 1.

According to FTIR studies of monomeric, micellular, and pure solid CTMAB and dried organic clay complexes (Kung and Hayes, 1993; Vaia *et al.*, 1994; Li and Ishida, 2003; Zhu *et al.*, 2005), the vibration bands at

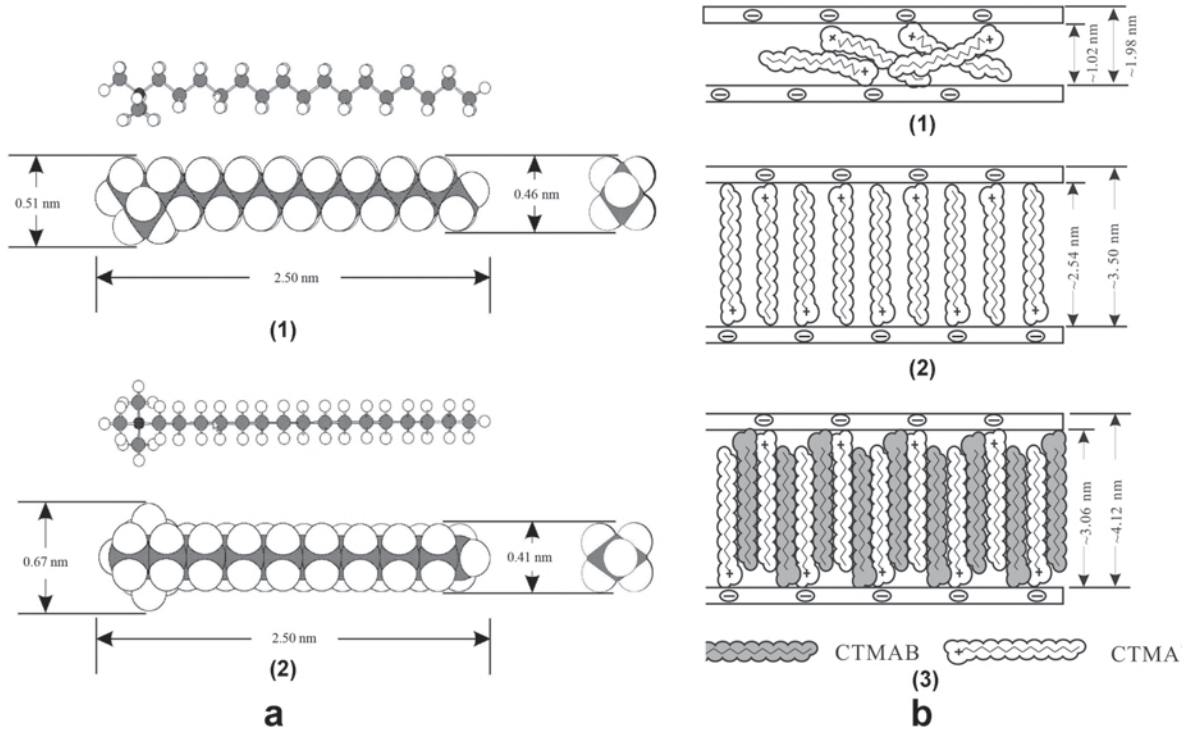

Figure 2. Dimensions of $CTMA^+$ and the intercalates sorbed in the interlayer space of organo-bentonite: (a1) side elevation; (a2) planform view; (b1) low surfactant loadings; (b2), middle surfactant loadings; (b3) large surfactant loadings.

2918 and 2850 cm^{-1} correspond to the C−H antisymmetric and symmetric alkyl-stretching modes, respectively. The shifts of these two bands have been interpreted in terms of the structural order of the methylene chain group, *i.e.* the shifts correlate with not only the *gauche/trans* conformation but also with the phase transformation between solid-like and liquid-like states. The band shifts from lower frequencies, characteristic of highly ordered, all-*trans* conformations, to higher frequencies and increases in width as the number of *gauche* conformations along the hydrocarbon chain (chain disorder) increases (Vaia *et al.*, 1994).

In order to understand the long-chain conformation of surfactant cations at different degrees of hydration, the C-H vibrations of the alkyl chains of the surfactant monomer, micelles, and intercalates were investigated. The monomer and the micelles were examined in aqueous solution below or above the critical micellar concentration (CMC) of CTAB, respectively. By comparing the C-H vibrations in the wet, solid, micellar, and monomeric states in water (Table 1), the following can be noted (Table 1): (1) generally, intercalates in wet organo-bentonite vibrate at lower wavenumber than monomers, indicating a more ordered conformation in the intercalates (Kung and Hayes, 1993); (2) except for sample 0.2CEC, the intercalates have a more ordered conformation and lower stretching vibrational energies compared to the micelles; (3) for the organo-bentonites, the two absorption bands shift from higher to lower wavenumber when the surfactant loading is increased. As a general rule, the wavenumber shift from higher to lower corresponds to reduction of vibrational energies and an increase in the ordering and compactness of the structure of the alkyl tail (Kung and Hayes, 1993; Vaia *et al.*, 1994). When the surfactant loading increases to 0.8CEC, the CH_2 vibrational energy almost equals that of neat CTMAB.

The *in situ* FTIR spectra indicated that there are no monomers in intercalates, and the surfactant intercalates have a more ordered and compact structure than the micelles at low surfactant sorption density. Furthermore, the intercalates in wet organic bentonites change from a liquid-like state to a solid-like state. This is consistent with the change from a disordered to an ordered phase in the interlayer space of dried organic bentonites.

Microstructure characteristics of intercalates

To understand the state of intercalates in the interlayer space of wet organic bentonite, the packing density and the volume of surfactant, the volume of water, and the ratio of organic molecular volume to that of water were assessed using the stoichiometry data, interlayer height, dimension of $CTMA^+$, and exact surfactant loading level. The calculation procedure is based on the assumption that the basal surfaces contributed most to the total surface area of the studied

clay, the interactions of the lateral surfaces being ignored (Yariv and Cross, 2002).

The unit-cell parameters used to define the planar unit-cell dimensions are a = 0.52 nm, b = 0.90 nm, the thickness of silicate layer is 0.96 nm and the basal spacing (d_L) can be obtained from XRD. The negative charge is 0.82 per unit cell. After exchange reaction, the parameters a and b remain unchanged for organic bentonite, while d_L increases gradually with the increase of surfactant loading. The interlayer spacing is Δd ($\Delta d = d_L - 0.96$), so the volume of interlayer space per unit cell (V_{IS}) is $a \times b \times \Delta d$. The number of surfactant molecules and/or cations (N), including molecules (N_{CTMAB}) and cations (N_{CTMA^+}), in each unit cell was obtained by the exact surfactant loading level $\times 0.82$. The molecular ratios of water to surfactant in the bentonite interlayer are expressed as $M_{H_2O/CTMA^+}$. Each $CTMA^+$ volume (V_{CTMA^+}) was estimated by means of the following equation (Patrick *et al.*, 1999):

$$V_{CTMA^+}\ (nm^3) = 0.054\ n_{CH_3} + 0.027\ n_{CH_2} = 0.62\ nm^3 \quad (1)$$

The volume of water (V_{H_2O}) can be obtained by subtracting the volume of surfactant (V_{CTMA^+}) from V_{IS}. The packing density of the intercalated organic phase (ρ) is obtained by:

$$\rho\ (g/cm^3) = (M_{CTMA^+} \times N_{CTMA^+} + M_{CTMAB} \times N_{CTMAB}) \times 10^{21}/(V_{IS} \times 6.02 \times 10^{23}) \quad (2)$$

M_{CTMA^+} (284.57 g/mol) and M_{CTMAB} (364.47 g/mol) are molar masses of $CTMA^+$ and CTMAB, respectively. Through the stoichiometry, the packing density in moist organic clay is obtained (shown in Table 2), ranging from 0.16 to 0.75 g/cm^3 with the increase in loading level. Compared with the density of the CTMAB crystal (0.96 g/cm^3), the intercalates in the interlayer space are, therefore, at best, quasi-crystalline even at the greatest surfactant loading.

The property of the surface is mainly governed by the extent of hydrophobicity, *i.e.* the ratio of induced hydrophobic sites (= $CTMA^+$) to indigenous hydrophilic sites (= inorganic interlayer cations or the polar water molecules). Therefore, the ratio of V_{H_2O} to V_{CTMA^+} and M_{H_2O} to M_{CTMA^+} can reflect, to a certain extent, the degree of hydration in the interlayer. As shown in Table 2, this ratio decreases in linear fashion with surfactant loading, and the volume percent of water, ratio of V_{H_2O} to V_{IS}, varies from 79% (0.2 CEC) to 14% (3.0CEC), and the molar ratio of water to sorbed surfactant decreases in a similar trend from 204.30 (0.2CEC) to 8.62 (3.0CEC). The latter reflects the change of clay surface affinity from hydrophilic to hydrophobic. In the range of 1.0−1.2CEC loading level, the volumes of surfactant and water are equal, and the corresponding organic bentonites display the greatest sorption coefficients.

The density of the interlayer organic phase (ρ) and the number of surfactant molecules per unit cell (N) increase with increase in interlayer spacing during the swelling process, but the volume fraction of water (V_{H_2O}/V_{IS}) in the interlayer has the opposite tendency. Three stages can be distinguished from the relationship between these parameters and the interlayer spacing (Δd) (Figure 3). At the first stage, Δd = 2.06 nm, N is doubled but ρ and V_{H_2O}/V_{IS} are unchanged for the 0.2CEC and 0.4CEC samples; this implies that the water and surfactant may be intercalated into the interlayer space in a specific proportion at the beginning of intercalation. At the second stage, 2.06 nm < Δd < 3.12 nm, ρ and N are increased gradually, but V_{H_2O}/V_{IS} decreases with increasing layer separation. At the third stage, $\Delta d \geqslant 3.12$ nm, ρ and N are increased sharply, and V_{H_2O}/V_{IS} decreases rapidly when the layer separation continues to increase. Knowing the amount of adsorbed surfactant and the amount of liquid intercalated, the variation of ρ, Δd, and N with the hydrophilicity of internal surface, expressed by the mole fraction of surfactant (M), is shown in Figure 4. ρ, N, and Δd increase with increasing values of M; ρ and N increase at a greater rate up to 1.60CEC (M<0.07) than after 1.60CEC (M>0.07). For Δd, there is little change after 1.60CEC (M>0.07), which means that the increment of surfactants in the interlayer has little effect on the interlayer swelling at large surfactant loadings.

Sorption of organic pollutants onto organic bentonites

To investigate the effect of a hydrophobic environment on sorption of organic pollutants in the interlayer space, sorption of nitrobenzene, phenol, and aniline onto CTMAB bentonites was investigated. Analogous to previous studies, the sorption coefficients (K_d) derived from the slopes of linear isotherms vary with different surfactant loading levels (Xu and Boyd, 1995; Sheng *et al.*, 1996a; Zhu *et al.*, 2003b; Slade and Gates, 2004a; Chen *et al.*, 2005). In the case of small surfactant loading

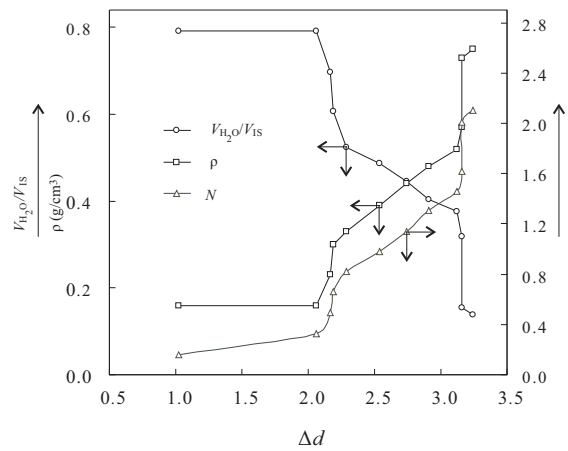

Figure 3. Variation in the density of the interlayer organic phase (ρ), the number of surfactant molecules and/or cations per unit cell (N), and the volume fraction of water (V_{H_2O}/V_{IS}) with the interlayer spacing.

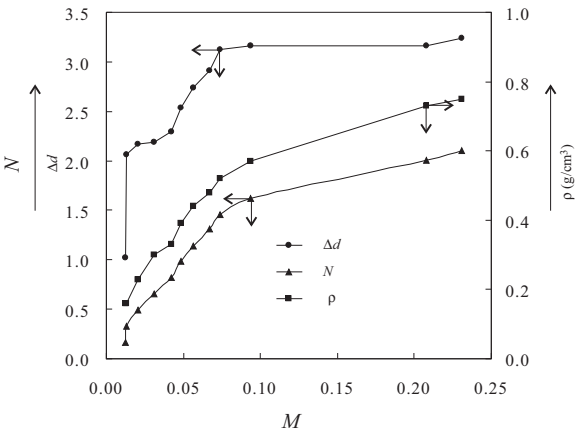

Figure 4. Variation of ρ, Δ*d*, and *N* with molar fraction of surfactant (*M*).

levels, the K_{sf} values, *i.e.* the carbon-normalized solute distribution coefficients of nitrobenzene, phenol, and aniline with CTMAB-bentonite, increase significantly with the increase in $CTMA^+$ and reach a maximum at ~1.0CEC. Thereafter, the K_{sf} values decrease sharply over the range 1.2−2.56CEC (Figure 5). Beyond 1.2CEC, a strong linear (negative) relationship could be seen between the quantity of adsorbed surfactant salt molecules and the K_{sf} values (Figure 5a). The K_{sf}/K_{ow} ratios, which ignored the effect of K_{ow} on solute distribution coefficients, were extremely large (Figure 5b) for aniline with its donor-electron group of $-NH_2$, followed by that of phenol. The smallest value is for nitrobenzene with the electron-attracting group $-NO_2$. These data further demonstrated the multiple properties of microenvironments in the clay interlayer.

The variation in K_{sf} with $CTMA^+$ level and synergistic sorption of organic bentonite is indicative of more than a single dominant sorption mechanism for the organo-clay in question. Li and Bowman (1998) suggested that, for a given f_{oc}, the sorption is reduced when the density of the bound organic phase increases. The results suggest that the sorption process is influenced by the loading level, composition, and configuration of the sorbed organic cation.

Steric hindrance

Potential arrangements of sorbed surfactant molecules are shown in Figure 6. Taking into account the vertical projection area per negative charge on the NM montmorillonite (~0.57 nm^2), the calculated diameter per negative charge (D_e) is ~0.86 nm. In the case of a small surfactant loading (Figure 6a), there is sufficient unoccupied space on the siloxane surface to accommodate both surfactant and organic contaminant due to the hydrophilic head, where the electric charge is concentrated, anchoring on the clay surface and then exposing the hydrophilic siloxane surface. When the exchangeable sites are completely occupied by $CTMA^+$ in the 1.0CEC sample (Figure 6b), the height of the interlayer permits surfactant cations to adopt an arrangement perpendicular to the silicate layer surface and the rod of the surfactant anchoring its head at the center of the electrostatic field. Thus, the spacing between the 'pillars' of $CTMA^+$ is 0.40−0.45 nm, obtained by subtracting the alkyl chain diameter (0.41−0.46 nm) from D_e, providing room for the surfactant molecules when the loading level is greater than the CEC.

The surfactant loading in the 3.0CEC sample is ~2.56 times the CEC. The surfactant salt molecules occupy the space between the $CTMA^+$ pillars when entering into the clay interlayer space (Figure 6c). Hence, the area occupied per molecule on the surface is ~0.22 nm^2, almost equal to the transverse cross-sectional area of the alkyl chain rod. In this case, the arrangement of CTMAB looks like matches stacked in a matchbox, with no space available for contaminants. Thus, the accessible volume for holding organic matter strongly on the organic bentonites with greater surfactant loading is reduced by the steric hindrances. This might be the main cause for the decrease in sorption capability of the organic bentonites with high surfactant loading.

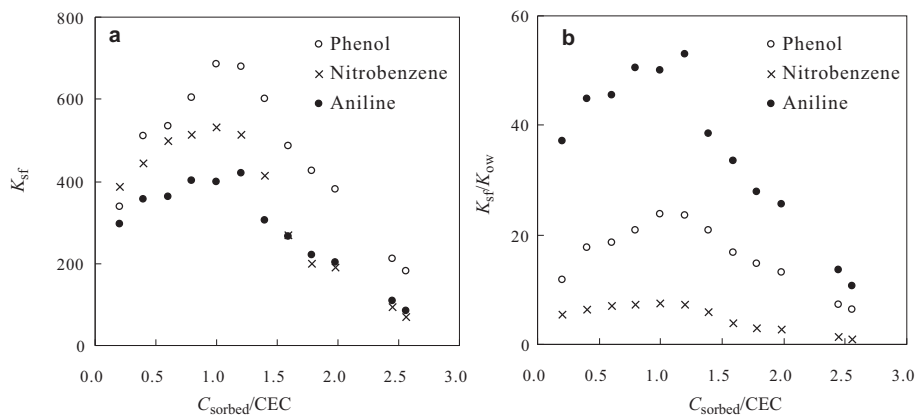

Figure 5. The relationship between sorption characteristics of the organic bentonites and levels of CTMAB sorbed (C_{sorbed}/CEC): the carbon-normalized solute sorption coefficients (K_{sf}) (a) and K_{sf}-normalized with K_{ow} (b).

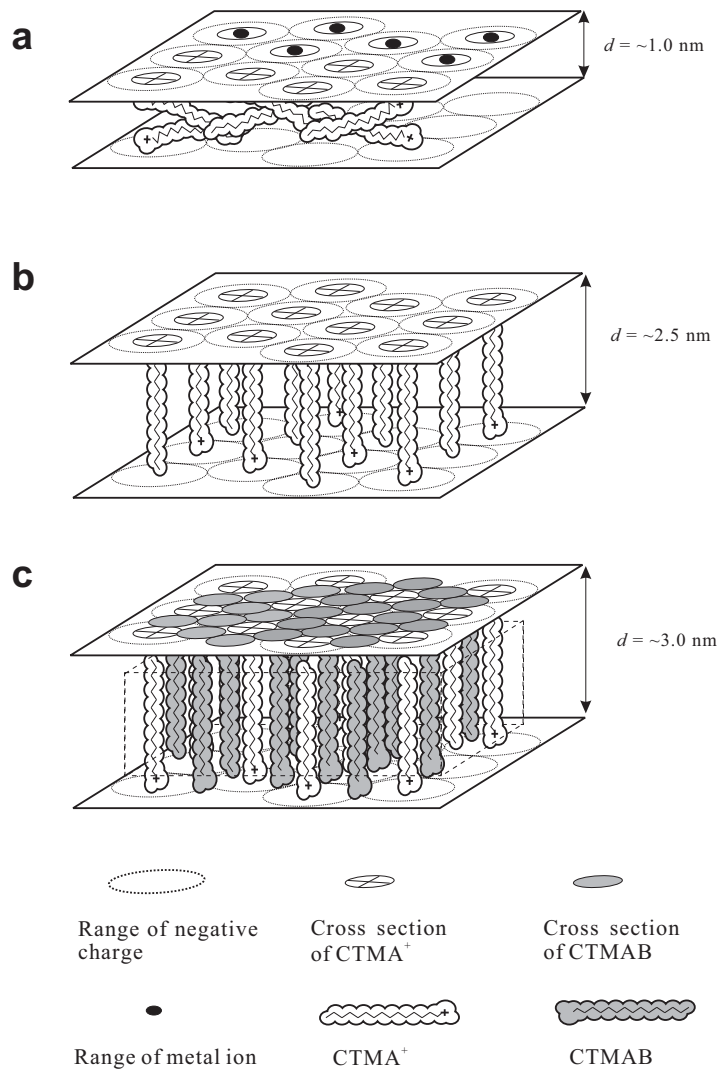

Figure 6. Schematic 3D drawing of locations of surfactant molecules and/or ions' locations on the clay layers (including the top view): (a) small surfactant loadings; (b) middling surfactant loadings (1.0CEC); (c) large surfactant loadings. (The dashed-line cube is given as the partition phase, and the available space confined by the hydrophobic siloxane surface is gradually reduced by the increases in surfactant loadings.)

To summarize, the structure and properties of intercalates on the internal interface of water-organic bentonites were restricted by the surfactant loading and differed from the organic phase in the dry organic bentonites. This research provides an explanation as to why surfactants with long alky chains sorbed on bentonite can reach only 2.5 times the CEC using the microstructure of 'solloids' and organic bentonites. Meanwhile, changes in the structure and properties parameters with increase in surfactant loading have been demonstrated. The results from this research indicate that the steric hindrances for the sorption of NOCs, occurring at large surfactant loadings, might be a negative factor in terms of the sorption capacity. This should be considered during the treatment of wastewater with organic bentonites.

ACKNOWLEDGMENTS

This work was funded by the National Natural Science Foundation of China (Grant No. 50378081, 40673077).

REFERENCES

Bakker, M.G., Morris, T.A., Tu, G.L. and Granger, E. (2000) Surfactant aggregates (solloids) adsorbed on silica as stationary chromatographic phases: structures and properties. *Journal of Chromatography B: Biomedical Sciences and Applications*, **743**, 65–78.

Boyd, S.A., Mortland, M.M., and Chiou, C.T. (1988) Sorption characteristics of organic compounds on hexadecyltrimethylammonium-smectite. *Soil Science Society of America Journal*, **52**, 652–657.

Chen, B.L., Zhu, L.Z., Zhu, J.X., and Xing, B.S. (2005) Configurations of the bentonite-sorbed myristylpyridinium cation and their influences on the uptake of organic

compounds. *Environmental Science & Technology*, **39**, 6093–6100.

Dékány, I. (1992) Liquid adsorption and immersional wetting on hydrophilic/hydrophobic solid surfaces. *Pure and Applied Chemistry*, **64**, 1499–1509.

Dékány, I. (1994) Interaction between surfactants and soil colloids: adsorption, wetting and structural properties. *Progress in Colloid and Polymer Science*, **95**, 73–90.

Dékány, I., Szanto, F., Nagy, L.G., and Foti, G. (1975) Adsorption of liquid mixtures on bentonite and organophilic bentonite. *Journal of Colloid and Interface Science*, **50**, 265–271.

Dékány, I., Szántó, F., Weiss, A., and Lagaly, G. (1985) Interlamellar liquid sorption on hydrophobic silicates. *Berichte der Bunsen-Gesellschaft Physical Chemistry Chemical Physics*, **89**, 62–67.

Dékány, I., Szántó, F., and Nagy, L.G. (1986a) Sorption and immersional wetting on clay minerals having modified surface. II. Interlamellar sorption and wetting on organic montmorillonites *Journal of Colloid and Interface Science*, **109**, 376–384.

Dékány, I., Szántó, F., Weiss, A., and Lagaly, G. (1986b) Interactions of hydrophobic layer silicates with alcohol-benzene mixtures. II. Structure and composition of the adsorption layer. *Berichte der Bunsen-Gesellschaft Physical Chemistry Chemical Physics*, **90**, 427–431.

Dékány, I., Szántó, F., and Weiss, A. (1989) The liquid-crystal structure of adsorbed layer and the stability of dispersed systems in organic liquids. *Colloids and Surfaces*, **41**, 107–121.

Dékány, I., Szekeres, M., Marosi, T., Balázs, J., and Tombácz, E. (1994) Interaction between surfactants and soil colloids: adsorption, wetting and structural properties. *Progress in Colloid and Polymer Science*, **95**, 73–90.

Dékány, I., Farkas, A., Kiraly, Z., Klumpp, E., and Narres, H.D. (1996) Interlamellar adsorption of 1-pentanol from aqueous solution on hydrophobic clay minerals. *Colloids and Surfaces, A: Physicochemical and Engineering Aspects*, **119**, 7–13.

Döring, J., Lagaly, G., Beneke, K., and Dékány, I. (1993) Interlamellar adsorption of alcohols. 4. Adsorption properties of crystalline silicas. *Colloids and Surfaces, A: Physicochemical and Engineering Aspects*, **71**, 219–231.

Fan, A.X., Somasundaran, P., and Turro, N.J. (1997) Adsorption of alkyltrimethylammonium bromides on negatively charged alumina. *Langmuir*, **13**, 506–510.

Favre, H. and Lagaly, G. (1991) Organo-bentonites with quaternary alkylammonium ions. *Clay Minerals*, **26**, 19–32.

Harwell, J.H. (1985) Pseudophase separation model for surfactant adsorption: isomerically pure surfactants. *Langmuir*, **1**, 251– 262.

He, H.P., Frost, R.L., Deng, F., Zhu, J.X., Wen, X.Y., and Yuan, P. (2004) Conformation of surfactant molecules in the interlayer of montmorillonite studied by ^{13}C MAS NMR. *Clays and Clay Minerals*, **52**, 350–356.

He, H.P., Galy, J., and Gerard, J.F. (2005) Molecular simulation of the interlayer structure and the mobility of alkyl chains in $HDTMA^+$/montmorillonite hybrids. *Journal of Physical Chemistry B*, **109**, 13301–13306.

Jaynes, W.F. and Boyd, S.A. (1991) Clay mineral type and organic compound sorption by hexadecyltrimethylammonium-exchanged clays. *Soil Science Society of America Journal*, **55**, 43–48.

Kung, K.H.S. and Hayes, K.F. (1993) Fourier-transform infrared spectroscopic study of the adsorption of cetyltrimethylammonium bromide and cetylpyridinium chloride on silica. *Langmuir*, **9**, 263–267.

Lagaly, G. (1976) Kink-block and crooked-block structures of bimolecular films. *Angewandte Chemie*, **88**, 628–639.

Lagaly, G. (1981) Characterization of clays by organic compounds. *Clay Minerals*, **16**, 1–21.

Lagaly, G. (1982) Layer charge heterogeneity in vermiculites. *Clays and Clay Minerals*, **30**, 215–222.

Lee, E.M., Thomas, R.K., Penfold, J., and Ward, R.C. (1989) Structure of aqueous decyltrimethylammonium bromide solutions at the air water interface studied by the specular reflection of neutrons. *Journal of Physical Chemistry*, **93**, 381–388.

Lee, S.Y. and Kim, S.J. (2002) Expansion of smectite by hexadecyltrimethylammonium. *Clays and Clay Minerals*, **50**, 435–445.

Li, Y.Q. and Ishida, H. (2003) Concentration-dependent conformation of alkyl tail in the nanoconfined space: hexadecylamine in the silicate galleries. *Langmuir*, **19**, 2479–2484.

Li, Z.H. and Bowman, R.S. (1998) Sorption of perchloroethylene by surfactant-modified zeolite as controlled by surfactant loading. *Environmental Science and Technology*, **32**, 2278–2282.

Marosi, T., Dékány, I., and Lagaly, G. (1994) Displacement processes on hydrophilic/hydrophobic surfaces in 1-propanol-water mixtures. *Colloid and Polymer Science*, **272**, 1136–1142.

Patrick, H.N., Warr, G.G., Manne, S., and Aksay, I.A. (1999) Surface micellization patterns of quaternary ammonium surfactants on mica. *Langmuir*, **15**, 1685–1692.

Rennie, A.R., Lee, E.M., Simister, E.A., and Thomas, R.K. (1990) Structure of a cationic surfactant layer at the silica-water interface. *Langmuir*, **6**, 1031–1034.

Sheng, G.Y. and Boyd, S.A. (2000) Polarity effect on dichlorobenzene sorption by hexadecyltrimethylammonium-exchanged clays. *Clays and Clay Minerals*, **48**, 43–50.

Sheng, G.Y., Xu, S., and Boyd, S.A. (1996a) Mechanism(s) controlling sorption of neutral organic contaminants by surfactant-derived and natural organic matter. *Environmental Science and Technology*, **30**, 1553–1557.

Sheng, G.Y., Xu, S.H., and Boyd, S.A. (1996b) Cosorption of organic contaminants from water by hexadecyltrimethylammonium-exchanged clays. *Water Research*, **30**, 1483–1489.

Slade, P.G. and Gates, W.P. (2004a) The swelling of HDTMA smectites as influenced by their preparation and layer charges. *Applied Clay Science*, **25**, 93–101.

Slade, P.G. and Gates, W.P. (2004b) The ordering of HDTMA in the interlayers of vermiculite and the influence of solvents. *Clays and Clay Minerals*, **52**, 204–210.

Somasundaran, P. and Huang, L. (2000) Adsorption/aggregation of surfactants and their mixtures at solid-liquid interfaces. *Advances in Colloid and Interface Science*, **88**, 179–208.

Somasundaran, P. and Kunjappu, J.T. (1989) In-situ investigation of adsorbed surfactants and polymers on solids in solution. *Colloids and Surfaces*, **37**, 245–268.

Szántó, F., Dékány, I., Patzkó, Á., and Várkonyi, B. (1986) Wetting, swelling and sediment volumes of organophilic clays. *Colloids and Surfaces A – Physicochemical and Engineering Aspects*, **18**, 359–371.

Theng, B.K.G., Newman, R.H., and Whitton, J.S. (1998) Characterization of an alkylammonium-montmorillonite-phenanthrene intercalation complex by carbon-13 nuclear magnetic resonance spectroscopy. *Clay Minerals*, **33**, 221–229.

Vaia, R.A., Teukolsky, R.K., and Giannelis, E.P. (1994) Interlayer structure and molecular environment of alkylammonium layered silicates. *Chemistry of Materials*, **6**, 1017–1022.

Wang, L.Q., Liu, J., Exarhos, G.J., Flanigan, K.Y., and Bordia, R. (2000) Conformation heterogeneity and mobility of

surfactant molecules in intercalated clay minerals studied by solid-state NMR. *Journal of Physical Chemistry B*, **104**, 2810–2816.

Wu, J., Harwell, J.H., and O'Rear, E.A. (1987) Two-dimensional reaction solvents: surfactant bilayers in the formation of ultrathin films. *Langmuir*, **3**, 531–537.

Xu, S.H. and Boyd, S.A. (1995) Cationic surfactant adsorption by swelling and nonswelling layer silicates. *Langmuir*, **11**, 2508–2514.

Xu, S.H., Sheng, G.Y., and Boyd, S.A. (1997) Use of organoclays in pollution abatement. *Advances in Agronomy*, **59**, 25–62.

Yariv, S. and Cross, H. (2002) *Organo-clay Complexes and Interactions*. Marcel Dekker, New York.

Zhang, Z.Z., Sparks, D.L., and Scrivner, N.C. (1993) Sorption and desorption of quaternary amine cations on clays. *Environmental Science and Technology*, **27**, 1625–1631.

Zhu, J.X., He, H.P., Guo, J.G., Yang, D., and Xie, X.D. (2003a) Arrangement models of alkylammonium cations in the interlayer of $HDTMA^+$ pillared montmorillonites. *Chinese Science Bulletin*, **48**, 368–372.

Zhu, L.Z., Chen, B.L., Tao, S., and Chiou, C.T. (2003b) Interactions of organic contaminants with mineral-adsorbed surfactants. *Environmental Science and Technology*, **37**, 4001–4006.

Zhu, J.X., He, H.P., Zhu, L.Z., Wen, X.Y., and Deng, F. (2005) Characterization of organic phases in the interlayer of montmorillonite using FTIR and C-13 NMR. *Journal of Colloid and Interface Science*, **286**, 239–244.

(*Received 10 April 2007; revised 28 November 2007; Ms. 0016; A.E. W.P. Gates*)